Biophysical Chemistry 244 (2019) 22–28

Contents lists available at ScienceDirect

Biophysical Chemistry

journal homepage: www.elsevier.com/locate/biophyschem

Rational cyclization-based minimization of entropy penalty upon the binding of Nrf2-derived linear peptides to Keap1: A new strategy to improve therapeutic peptide activity against sepsis

Ke Chen[a,*], Liuliu Huang[b], Bin Shen[c]

[a] Department of Emergency, Liyang People's Hospital, Liyang 213300, China
[b] Department of Respiratory Medicine, Liyang Chinese Medicine Hospital, Liyang 213300, China
[c] Department of Emergency, Jiangsu Provincial People's Hospital, Nanjing Medical University, Nanjing 210029, China

HIGHLIGHTS

- Linear peptides derived from Nrf2–Keap1 binding site exhibit self-inhibitory activity.
- The peptides possess large flexibility in unbound state, and thus would incur a considerable entropy penalty upon binding.
- Peptide cyclization strategy is described to minimize the unfavorable entropy penalty.
- Cyclization can improve peptide affinity by 1.4–7.5-fold for designed cyclic peptides relative to their linear counterparts.

GRAPHICAL ABSTRACT

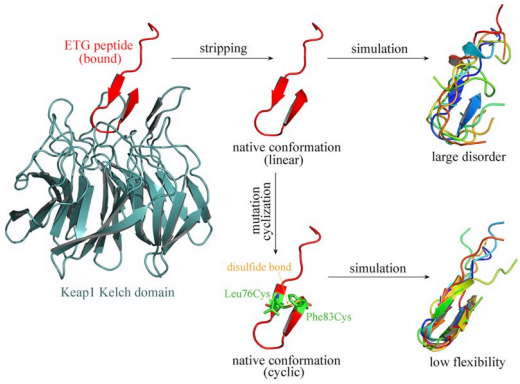

ARTICLE INFO

Keywords:
Keap1
Nrf2
Peptide
Cyclization
Entropy penalty
Sepsis

ABSTRACT

Nrf2 is a critical regulator of innate immune response and survival during sepsis, which is constitutively degraded through binding to the Keap1 adapter protein of E3 ubiquitin ligase. Two linear peptides DLG and ETG derived from, respectively, the low-affinity and high-affinity motifs of Nrf2 binding site exhibit self-binding affinity to Keap1 central hole (active pocket); they can be exploited as therapeutic self-inhibitory peptides to disrupt the Nrf2–Keap1 interaction. Molecular dynamics simulation and binding energetics decomposition reveal that the two peptides possess large flexibility and intrinsic disorder in unbound free state, and thus would incur a considerable entropy penalty upon binding to Keap1. In order to improve Keap1–peptide binding affinity (or free energy ΔG), instead of traditionally increasing favorable enthalpy contribution (ΔH) we herein describe a rational peptide cyclization strategy to minimize unfavorable entropy penalty (ΔS) upon the binding of Nrf2-derived linear peptides to Keap1. Crystal structure analysis impart that the native active conformations of DLG and ETG peptides bound with Keap1 are folded into *U*-shape and hairpin configurations, respectively, and adopt their turning head to insert into the central hole of Keap1. Here, cyclization is designed by adding a disulfide bond across the two arms of DLG *U*-shape or ETG hairpin, which would not influence the direct intermolecular interaction between Keap1 and peptide as well as desolvation effect involved in the interaction, but can effectively constrain the conformational flexibility and disorder of the two peptides in free state, thus largely minimizing entropy penalty upon the binding. Both free energy calculation and binding affinity assay

* Corresponding author.
E-mail address: kecchen@yeah.net (K. Chen).

https://doi.org/10.1016/j.bpc.2018.11.002
Received 25 October 2018; Received in revised form 11 November 2018; Accepted 12 November 2018
Available online 14 November 2018

substantiate that the cyclization, as might be expected, can moderately or considerably enhance peptide binding potency to Keap1, with affinity (dissociation constant K_d) increase by 1.4–7.5-fold for designed cyclic peptides relative to their linear counterparts.

1. Introduction

Sepsis is a clinical syndrome that has physiological, biological and biochemical abnormalities caused by a dysregulated inflammatory response to infection [1]. It is a leading cause of death in intensive care units with mortality rates that range between 30 and 70%, and the mortality rate is especially high in patients with nosocomial infections [2]. The Nrf2 (nuclear factor/erythroid 2-related factor 2) regulates a pleiotropic cytoprotective defense program including antioxidants and protects against septic inflammatory disorders by inhibiting oxidative tissue injury [3], which is a critical regulator of the innate immune response and survival during sepsis [4]. Under normal conditions, Nrf2 is constitutively degraded through binding to Keap1 (Kelch-like ECH-associated protein 1), an adapter protein of E3 ubiquitin ligase [5]. In the presence of oxidative and xenobiotic stresses, Nrf2 degradation is stalled, leading to a rapid accumulation of Nrf2. Nrf2 then translocates into the nucleus and binds to the regulatory regions of target genes to upregulate their transcription [6].

The regulatory system of Nrf2 activity has turned out as an attractive therapeutic target for sepsis syndrome due to its sophisticated mechanism [7]. Enhancing Nrf2 pathway by disruption of Keap1 in myeloid leukocytes has been found to protect against sepsis [8]. Over the past decades, a number of small-molecule compounds have been discovered to target the Keap1-mediated degradation of Nrf2 and cause Nrf2 accumulation [9]. However, the binding of Keap1 to Nrf2 is a typical protein–protein interaction (PPI) that normally has a wide, flat interface, for which classical small molecules are not always ideally suited to disrupt [10]. Instead, biologic drugs such as peptide inhibitors have been successfully exploited as promising disruptors of Nrf2–Keap1 interaction, which possess better PPI-targeting capability as compared to small-molecule inhibitors [11]. Previously, it was found that peptide segments derived from the binding site of Nrf2 exhibit self-binding affinity towards Keap1 [12,13]; these segments are known as self-inhibitory peptides or self-binding peptides [14–16] that are expected to block Nrf2–Keap1 interaction by rebinding at the interaction interface. In order to improve the binding affinity and biological activity of self-inhibitory peptides, some molecular methods such as natural residue mutation and unnatural amino acid substitution have been used to modify the peptide sequence and structure, thus directly improving enthalpy contribution (ΔH) to the binding free energy (ΔG) of modified peptides to Keap1 [17,18]. Here, instead of traditionally increasing favorable enthalpy contribution (ΔH) we described a rational peptide cyclization strategy to minimize unfavorable entropy penalty (ΔS) upon the binding of Nrf2-derived linear peptides to Keap1. The structural basis, energetic property and dynamic behavior of Keap1 interaction with both linear and cyclic peptides were investigated systematically. We also performed fluorescence-based assays to determine the binding affinity of rationally designed cyclic peptides to recombinant human Keap1, which were utilized to substantiate the findings and conclusions obtained from computational modeling, analysis and design.

2. Materials and methods

2.1.1. Setup of Keap1–Nrf2 peptide complex crystal structures

Nrf2 protein harbors two Keap1-binding motifs (DLG and ETG) at its N-terminal domain [19]. Intermolecular recognition and interaction between the two motifs and Keap1 Kelch domain constitute a key regulatory nexus for cellular Nrf2 activity through the formation of a two-site binding hinge-and-latch mechanism [20]. The DLG

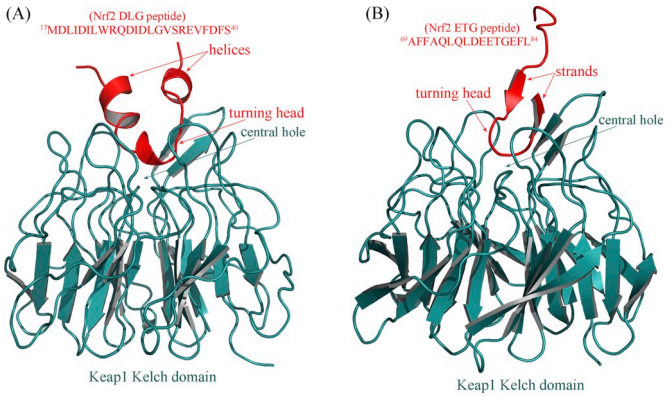

Fig. 1. Crystal structure of Keap1 Kelch domain in complex with the DLG (A) and ETG (B) peptides derived from Nrf2 N-terminal domain (PDB: 3WN7 and 4IFL, respectively).

(^{17}MDLIDILWRQDIDLGVSREVFDFS^{40}) and ETG (^{69}AFFAQLQLDEETGEFL^{84}) peptides separately derived from the two Keap1-binding motifs of Nrf2 N-terminal domain were co-crystallized with the Keap1 Kelch domain and deposited in the PDB database [21] with accession codes 3WN7 and 4IFL, respectively (Fig. 1). Here, the co-crystallized water molecules, organic ions and other cofactors were manually removed from the raw crystal structures; hydrogen atoms and protonation state were automatically assigned for the structures [22–24].

2.1.2. Molecular dynamics simulation

Molecular dynamics (MD) simulations of the investigated systems of proteins, peptides or their complexes were carried out with AMBER ff03 force field [25] implemented using the Amber biomolecular simulation programs [26]. All the systems were immersed in a truncated octahedral box of TIP3P water molecules [27] and Na^+ ions were added to obtain electrostatic neutrality. First, each system was minimized by applying harmonic restraints with a force constant of 10 kcal·mol^{-1}·Å^{-2} to all protein atoms, and then allowing all atoms to move freely [28]. The energy minimization was performed by the steepest descent method for the first 500 steps and the conjugated gradient method for the subsequent 2500 steps, which was followed by heating from 10 to 300 K over 100 ps in the canonical ensemble. Subsequently, MD production simulations (500-ns for peptides and 50-ns for complexes) were performed in an isothermal isobaric ensemble with periodic boundary conditions [29,30]. For all simulations, 2 fs time step and 10 Å nonbonded cutoff were used. The particle mesh Ewald method [31] was employed to treat long-range electrostatics, and bond lengths involving bonds to hydrogen atoms were constrained using the SHAKE algorithm [32].

Coordinates of the different conformations generated during the simulations were registered every 0.1 ns for a total of 500 snapshots per system, which were then used to calculate the complex binding energy ΔG with molecular mechanics/Poisson-Boltzmann surface area (MM/PBSA) method [33]:

$$\begin{aligned}\Delta G &= \Delta H - T\Delta S \\ &= \Delta E_{\text{int}} + \Delta D_{\text{dslv}} - T\Delta S\end{aligned} \quad (1)$$

where ΔE_{int} is the interaction energy between Keap1 and peptide, and ΔD_{dslv} is the desolvation effect and computed by numerical solution of nonlinear Poisson-Boltzmann equation plus surface area model [34]. The normal mode analysis (NMA) was performed to estimate the vibrational component of entropy [35]. Frequencies of the vibrational

modes were computed at 300 K for conformational snapshots and using a harmonic approximation of the energies [36].

2.1.3. Fluorescence polarization assay

The linear peptides were synthesized using Fmoc solid phase chemistry. For cyclic peptides, the sulhydryl groups of cysteine residues in reduced peptides were oxidized in 0.1 M ammonium bicarbonate to form disulfide bond between them [37]. The binding affinity of peptide ligands to Keap1 protein was determined using a fluorescence polarization (FP) protocol modified from previous reports [38,39]. The recombinant Keap1 protein was titrated to 50 nM FITC-labeled peptides in a buffer containing 50 mM HEPES (pH 7.4), 100 mM NaCl, 0.1% Tween-20 and 5 mM DTT. For cyclic peptides the DTT was not used to avoid disulfide bond reduction. A PE fluorescence spectrophotometer was utilized to monitor FP change upon the titration, and the dissociation constants (K_d) were derived by curve fitting [40]:

$$FP_{obs} = FP_0 + \frac{(FP_\infty - FP_0) \times [Keap1]}{K_d + [Keap1]} \quad (2)$$

where FP_{obs} is the observed FP value, FP_0 is the value of the free peptide, FP_∞ is maximum value of the completely bound peptide, and [Keap1] is the total Keap1 protein concentration titrated to peptide buffer solution.

3. Results and discussion

3.1.1. Nrf2-derived linear peptides are highly flexible

The Keap1 Kelch domain consists of six Kelch repeats, which are packed together in a knobs-into-holes manner to form a penetrating pocket as the accommodative site of two distinct binding motifs within the Nrf2 N-terminal domain, namely, the low-affinity DLG motif and the high-affinity ETG motif [41]. This two-site binding mode of Nrf2 to Keap1 allows for the efficient ubiquitination of Nrf2 since there are seven lysine residues between the DLG and ETG motifs [42]. The two motifs can be exploited as self-inhibitory peptides (SIPs) [14], which are expected to be able to rebind at Keap1–Nrf2 complex interface and then competitively disrupt the native complex interaction. The DLG and ETG motifs are two 24-mer and 16-mer peptide segments that cover the residues 17–40 and 69–84 of Nrf2 N-terminal domain, respectively. Visual analysis of the co-crystallized complex structures of Keap1 Kelch domain with the two peptide segments (PDB: 3WN7 and 4IFL) revealed that the DLG peptide is folded into a partially helical conformation, while the ETG peptide forms as a two-stranded conformation (Fig. 1). A considerable region of the two peptides has no defined structural feature; both of them adopt their turning heads to insert into the Keap1 central hole (active pocket) surrounded by six Kelch repeats.

The native active conformations of linear DLG and ETG peptides were taken from the co-crystallized complex structures and then separately subjected to 500-ns MD simulations to investigate their conformational flexibility and thermal motion in free state (Fig. 2). The backbone root-mean-square deviation (RMSD) fluctuation profiles of the two peptides during the whole simulations were examined, where their dynamic snapshots were extracted at 0, 100, 200, 300, 400 and 500 ns of the simulation trajectory. As seen, a strong RMSD oscillation can be observed through the whole simulation procedure (Fig. 2A), indicating that the two peptides are intrinsically disordering with large flexibility. Conformational analysis also supported this finding; the native structured conformations (helices for DLG peptide and strands for ETG peptide) are fast unfolded within the initial 100-ns simulations and all these conformational snapshots are vulnerable and exhibit high variability (Fig. 2B), thus unable to maintain in the native active conformations as their location in the context of Keap1–Nrf2 complex interface — this is unfavorable for the two linear peptides to rebind at the complex interface.

The total binding free energy ΔG of DLG and ETG peptide ligands to Keap1 Kelch domain receptor was calculated using MM/PBSA and NMA analysis based on 500 structural snapshots extracted from the dynamics trajectory of 50-ns MD production simulations of the domain–peptide complexes. The ΔG value can be decomposed into the intermolecular interaction energy ΔE_{int} between domain and peptide, the desolvation effect ΔD_{dslv} incurring from the interaction, and the entropy penalty $-T\Delta S$ upon the interaction *via* a statistical modeling approach [43–45]. The decomposed energetic components were listed in Table 1. The ΔE_{int} values were calculated as −284.3 and − 195.6 kcal/mol for DLG and ETG peptides, respectively, indicating that the direct interaction enthalpy is very favorable for the domain–peptide binding. However, the favorable ΔE_{int} would be largely impaired by the unfavorable desolvation (ΔD_{dslv} = 211.6 and 126.2 kcal/mol, respectively) and entropy penalty ($-T\Delta S$ = 60.9 and 45.8 kcal/mol, respectively). Consequently, the two peptide ligands can only bind to Keap1 with a moderate potency due to their high hydrophilicity and large flexibility. Subsequently, the linear DLG and ETG peptides were synthesized by solid phase chemistry, and their binding affinity to the recombinant protein of human Keap1 was measured using fluorescence polarization assays. As might be expected, the two peptides were determined as moderate binders of Keap1 (K_d = 380 and 23 nM, respectively). Consistently, the high-affinity ETG motif can bind tighter than the low-affinity DLG motif (~17-fold).

3.1.2. Cyclization can improve Nrf2-derived peptide affinity

Crystallographic analysis revealed that the DLG and ETG peptides can form *U*-shape configuration and hairpin configuration in native co-crystallized complexes with Keap1 Kelch domain, respectively, and use their turning head to insert into the domain's active pocket [46]. Here, considering that both the peptide ligands and domain pocket are highly polar and a complicated hydrogen-bonding network can be formed at their complex interface (Fig. 3) [47], direct mutation or modification of

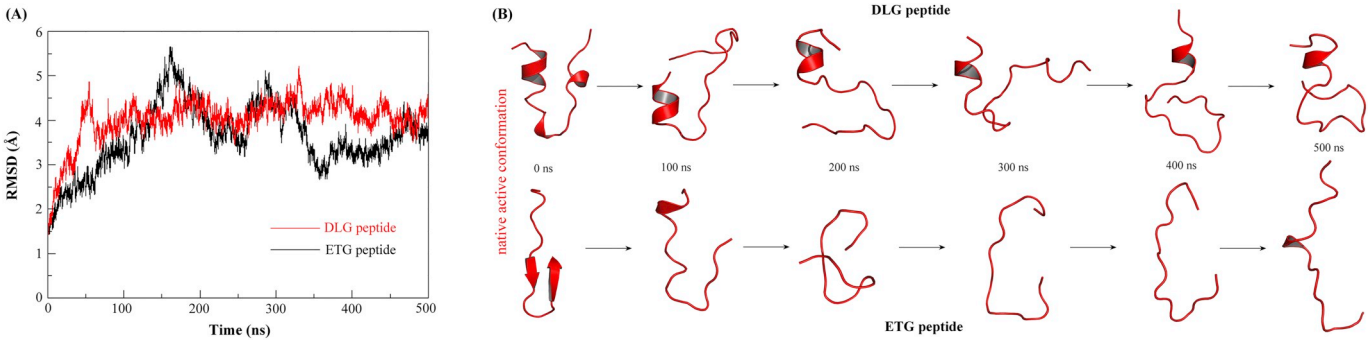

Fig. 2. 500-ns MD simulations of linear DLG and ETG peptides in free state. Their native active conformations taken from crystal complex structures were used as the start (0 ns) to perform the simulations. (A) The backbone RMSD fluctuation profiles of DLG and ETG peptides during the simulations. (B) The conformational snapshots of the two linear peptides are taken at 0, 100, 200, 300, 400 and 500 ns of the simulations.

Table 1
The binding energetics and affinity of linear and cyclized DLG and ETG peptides to Keap1 Kelch domain.

Peptide	Type	Sequence	Energetics (kcal/mol)				Affinity K_d (nM)
			ΔE_{int}	ΔD_{dslv}	$-T\Delta S$	ΔG	
DLG	Linear	^{17}MDLIDILWRQDIDLGVSREVFDFS^{40}	−284.3	211.6	60.9	−11.8	380 ± 64
DLG(cyc20–38)	Cyclic	^{17}MDLCDILWRQDIDLGVSREVFCFS^{40}	−275.2	218.3	32.6	−24.3	51 ± 8 (7.5-fold)[a]
DLG(cyc23-37)	Cyclic	^{17}MDLIDICWRQDIDLGVSREVCDFS^{40}	−266.3	210.2	38.7	−17.4	n.d.[b]
DLG(cyc24-34)	Cyclic	^{17}MDLIDILCRQDIDLGVSCEVFDFS^{40}	−270.5	216.3	34.6	−19.8	276 ± 52 (1.4-fold)[a]
ETG	Linear	^{69}AFFAQLQLDEETGEFL^{84}	−195.6	126.2	45.8	−23.6	23 ± 5
ETG(cyc75–84)	Cyclic	^{69}AFFAQLCLDEETHGEFC^{84}	−182.4	124.1	29.8	−28.5	6 ± 1 (3.8-fold)[a]
ETG(cyc76-83)	Cyclic	^{69}AFFAQLQCDEETGECL^{84}	−174.0	110.8	32.5	−30.7	12 ± 2 (1.9-fold)[a]

[a] the affinity increase fold of cyclic peptides relative to their linear counterparts.
[b] n.d., not detectable.

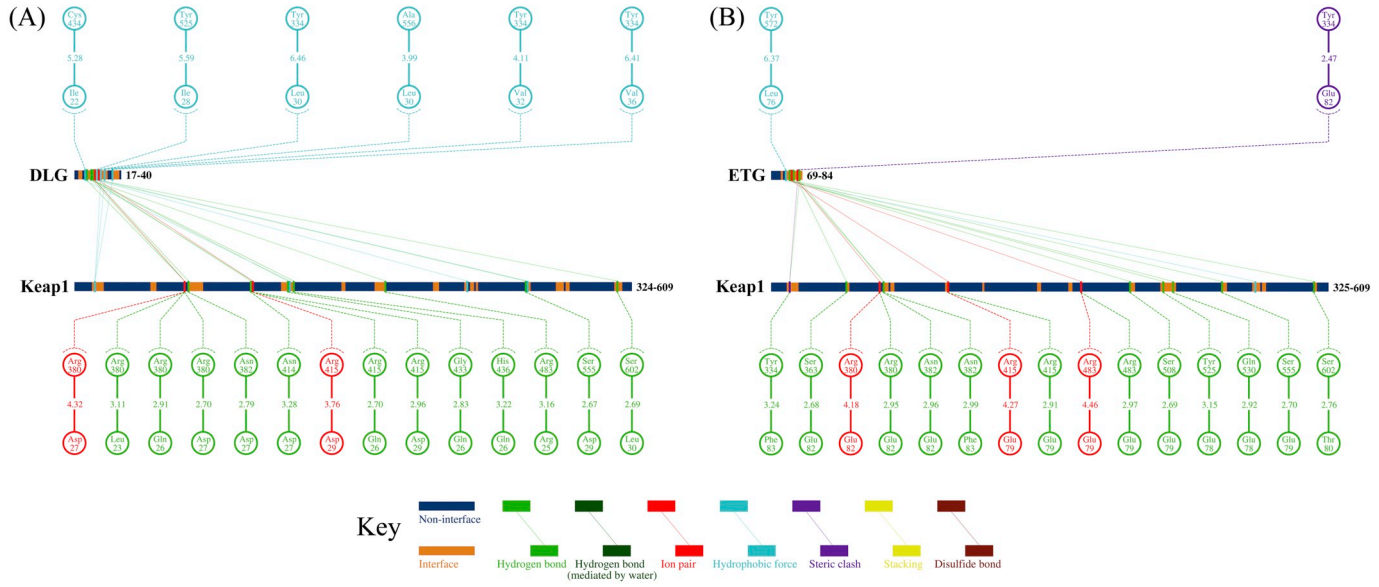

Fig. 3. Schematic representation of hydrogen bonds and other nonbonded forces at the complex interface of Keap1 Kelch domain with DLG (A) and ETG (B) peptides. The plot was generated using 2D-GraLab [47] based on their crystal complex structures (PDB: 3WN7 and 4IFL, respectively).

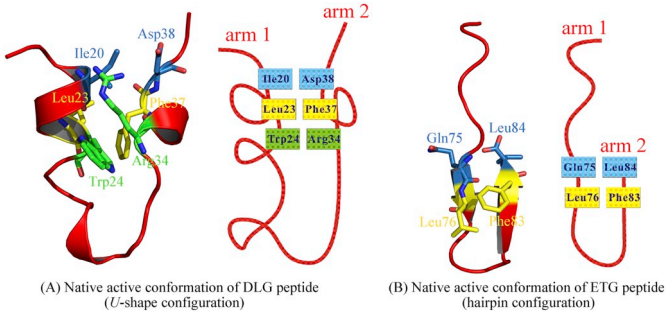

(A) Native active conformation of DLG peptide (*U*-shape configuration)
(B) Native active conformation of ETG peptide (hairpin configuration)

Fig. 4. The native active conformations of both the DLG (A) and ETG (B) peptides are folded into a *U*-shape hairpin configuration. The arm 1 residues Ile20, Leu23 and Trp24 are spatially vicinal to the arm 2 residues Asp38, Phe37 and Arg34 of DLG hairpin, respectively, while the arm 1 residues Gln75 and Leu76 are spatially vicinal to the arm 2 residues Leu84 and Phe83 of ETG hairpin, respectively.

peptide residues may undermine the established hydrogen bonds and other nonbonded forces, thus unfavorable to enthalpy (ΔH) involved in the complex interaction. Instead, above MD simulations suggested that the two linear peptides cannot maintain the native *U*-shape hairpin configuration in free state, and exhibit a large flexibility and intrinsic disorder during the whole simulation course, thus incurring a considerable entropy penalty upon binding to Keap1 Kelch domain. The entropy penalty was previously defined as indirect readout in protein–peptide recognition, which can be considered as a different story from classical biomolecular recognition [48]. Molecular analysis and characterization of entropy effect have been successfully used to study protein–peptide binding phenomena [49–51]. Recently, the head-to-tail cyclic peptides and intracyclic conformations have been reported to optimize potent Keap1–Nrf2 peptide inhibitors [52,53]. Here, we considered to cyclize the peptides by adding a disulfide bond across the two arms of *U*-shape hairpin. In this way, the conformational flexibility of unbound peptides should be largely reduced, thus minimizing entropy penalty upon the complex binding.

Visual examination of the native active conformation of DLG and ETG peptides revealed that there are a number of residue pairs across the two arms of peptides that (i) they are spatially vicinal to each other and (ii) their side chains do not form effective interactions with Keap1 protein receptor, including three residue pairs Ile20-Asp38, Leu23-Phe37 and Trp24-Arg34 for DLG peptide as well as two residue pairs Gln75-Leu84 and Leu76-Phe83 for ETG peptide (Fig. 4). Therefore, disulfide bond was considered to bridge across these residue pairs with a small influence on the native conformation of peptides. In the procedure, the two residues in a pair were mutated to Cys when disulfide bond is formed across them. The two peptides do not contain wild-type cysteine and thus can avoid mismatched disulfide bond in cyclic

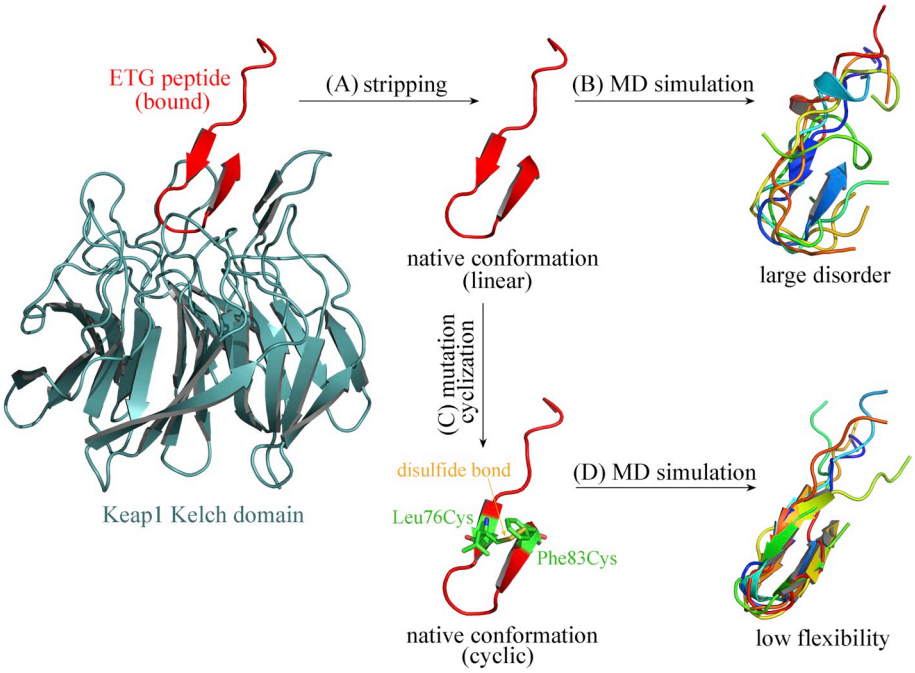

Fig. 5. An example of cyclization-improved peptide rigidity. (A) The EGT peptide is stripped from its crystal complex structure (PDB: 4IFL) with Keap1 Kelch domain to obtain the peptide native conformation. (B) The free EGT peptide is then subjected to MD simulations, during which the linear peptide displays a large disorder. (C) The spatially vicinal residues Leu67 and Phe83 of EGT peptide are mutated to Cys67 and Cys83, respectively, and a disulfide bond is formed across them to cyclize the peptide. (D) The resulting cyclic ETG(cyc67–83) peptide is then re-subjected to MD simulations, during which the cyclic peptide is relative rigid and can maintain in a two-stranded structure close to its native active conformation.

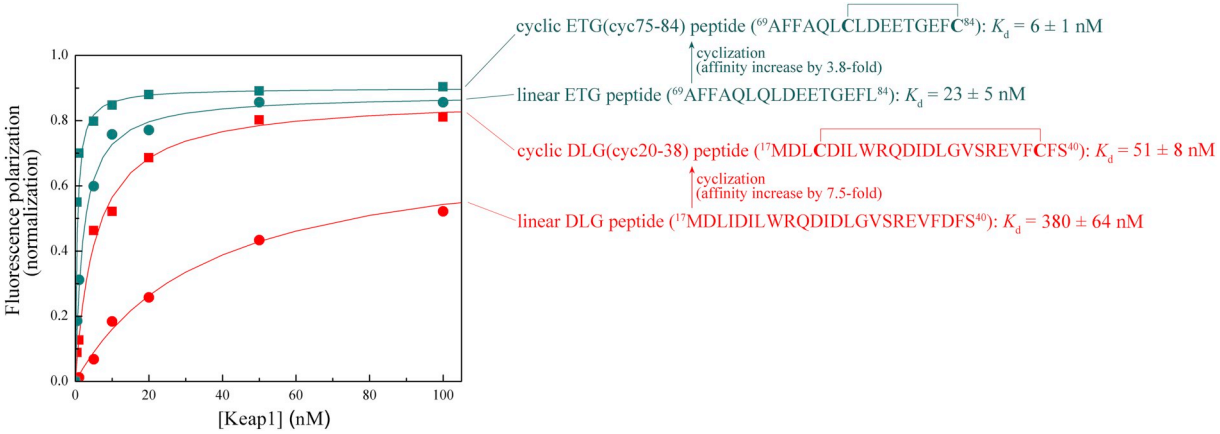

Fig. 6. The fluorescence polarization curve change from linear DLG and ETG peptides to their cyclic counterparts DLG(cyc20–38) and ETG(cyc75–84), respectively.

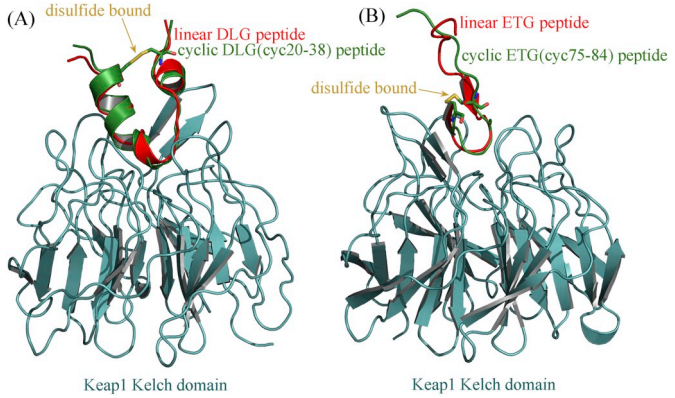

Fig. 7. Superposition of cyclic DLG(cyc20–38) and ETG(cyc75–84) peptides onto linear DLG and ETG peptides in the active pocket of Keap1 Kelch domain, respectively, where the bound conformations of both the linear and cyclic peptides in complex with Keap1 Kelch domain are reached at equilibrium with MD simulations.

peptide synthesis. Consequently, totally three cyclic DLG peptides and two cyclic ETG peptides were obtained based on the disulfide bond-formed cyclization between these candidate residue pairs (Table 1).

The cyclization across N-terminal residue Leu76 (arm 1) and C-terminal residue Phe83 (arm 2) of DLG peptide is schematically shown in Fig. 5. The linear DLG peptide was stripped from its crystal complex structure with Keap1 Kelch domain to obtain the peptide native conformation (A). The conformation was then subjected to 500-ns MD simulations (B), and a large flexibility and intrinsic disorder of the peptide was observed during the simulations. This is consistent with above analysis. The residues Leu76 and Phe83 were mutated to Cys76 and Cys83, respectively, and a disulfide bond was formed across them to cyclize the peptide (C). The resulting cyclic peptide ETG(cyc76–83) was re-subjected to 500-ns MD simulations, during which the cyclic peptide is relatively rigid and can maintain in a two-stranded structured configuration close to its native active conformation (D).

Similarly, other four cyclic peptides DLG(cyc20–38), DLG(cyc23–37), DLG(cyc24–34) and ETG(cyc75–84) can be obtained *via* the cyclization, and their binding energetics to Keap1 Kelch domain were calculated using MM/PBSA and NMA analysis (Table 1). As might be expected, the cyclization can indeed improve the binding capability

of DLG and ETG peptides as compared to their linear counterparts, with ΔG change from −11.8 kcal/mol to −24.3, −17.4 and − 19.8 kcal/mol (for three cyclic DLG peptides) as well as from −23.6 kcal/mol to −28.5 and − 30.7 kcal/mol (for two cyclic ETG peptides). Binding energy decomposition revealed that the entropy penalty is reduced considerably due to the cyclization, with $-T\Delta S$ decrease from 60.9 kcal/mol to 32.6, 38.7 and 34.6 kcal/mol (for three cyclic DLG peptides) as well as from 45.8 kcal/mol to 29.8 and 32.5 kcal/mol (for two cyclic ETG peptides), while the interaction energy ΔE_{int} and desolvation effect ΔD_{dslv} are changed moderately or modestly upon the cyclization (Table 1), suggesting that the cyclization primarily influences the conformation and flexibility of peptide ligands in free state, but has only a small effect on the direct intermolecular interaction of Keap1 with the peptides.

In order to substantiate the computational design, the binding affinity of five cyclic peptides to recombinant human Keap1 protein was measured using fluorescence polarization, and obtained K_d values are listed in Table 1. Consistently, cyclization can effectively improve binding affinity by 1.4–7.5-fold for four out of the 5 tested cyclic peptides (K_d = 51, 276, 6 and 12 nM) relative to their linear counterparts (K_d = 380 and 23 nM), although the cyclic peptide DLG(cyc23–37) has no observable affinity (K_d = n.d.) — this is not unexpected because some other factors such as atomic overlapping and steric collision induced by the cyclization may not be accurately described in theoretical modeling and may cause error and bias to the results. In five tested samples, the cyclic peptides DLG(cyc20–38) and ETG(cyc75–84) are considered as a good candidates since they possess high affinity (K_d = 51 and 6 nM, respectively) and exhibit a substantial affinity improvement (by 7.5-fold and 3.8-fold, respectively). Here, the binding curves of DLG(cyc20–38) and ETG(cyc75–84) as well as their linear counterparts DLG and ETG are plotted in Fig. 6. Evidently, the conformational constraint by cyclization can essentially shift the polarization curves of the two peptides binding to Keap1 (K_d change from 38.0 to 5.1 μM for DLG peptide and from 23 to 6 nM for ETG peptide), indicating a substantial effect of the cyclization on Keap1–peptide binding affinity.

The binding modes of designed high-affinity cyclic peptides DLG(cyc20–38) and ETG(cyc75–84) to Keap1 Kelch domain were modeled and equilibrated with 50-ns MD simulations, which were superposed onto the native active conformations of their respective linear counterparts (DLG and ETG) in crystal complex structures with the domain. By comparison it is readily observed that the binding modes of cyclic peptides are very similar to their native conformations, with root-mean-square deviation (RMSD) of 0.32 and 0.57 Å between their non-hydrogen atoms (Fig. 7), suggesting that the two cyclic peptides can bind in a similar manner to Keap1 as them in linear form. As designed, the disulfide bound is out of Keap1–peptide interaction pocket and hence would not disrupt the interaction.

Conflict of interest

All the authors declare that there are no conflicts of interest.

References

[1] N.C. Riedemann, R.F. Guo, P.A. Ward, Novel strategies for the treatment of sepsis, Nat. Med. 9 (2003) 517–524.

[2] C. Alberti, C. Brun-Buisson, H. Burchardi, C. Martin, S. Goodman, A. Artigas, A. Sicignano, M. Palazzo, R. Moreno, R. Boulmé, E. Lepage, R. Le Gall, Epidemiology of sepsis and infection in ICU patients from an international multicentre cohort study, Intensive Care Med. 28 (2002) 108–121.

[3] S.M. Ahmed, L. Luo, A. Namani, X.J. Wang, X. Tang, Nrf2 signaling pathway: pivotal roles in inflammation, Biochim. Biophys. Acta Mol. basis Dis. 1863 (2017) 585–597.

[4] R.K. Thimmulappa, H. Lee, T. Rangasamy, S.P. Reddy, M. Yamamoto, T.W. Kensler, S. Biswal, Nrf2 is a critical regulator of the innate immune response and survival during experimental sepsis, J. Clin. Invest. 116 (2006) 984–995.

[5] Z. Sun, S. Zhang, J.Y. Chan, D.D. Zhang, Keap1 controls postinduction repression of the Nrf2-mediated antioxidant response by escorting nuclear export of Nrf2, Mol. Cell. Biol. 27 (2007) 6334–6349.

[6] E.H. Kobayashi, T. Suzuki, R. Funayama, T. Nagashima, M. Hayashi, H. Sekine, N. Tanaka, T. Moriguchi, H. Motohashi, K. Nakayama, M. Yamamoto, Nrf2 suppresses macrophage inflammatory response by blocking proinflammatory cytokine transcription, Nat. Commun. 7 (2016) 11624.

[7] T. Suzuki, H. Motohashi, M. Yamamoto, Toward clinical application of the Keap1–Nrf2 pathway, Trends Pharmacol. Sci. 34 (2013) 340–346.

[8] X. Kong, R. Thimmulappa, F. Craciun, C. Harvey, A. Singh, P. Kombairaju, S.P. Reddy, D. Remick, S. Biswal, Enhancing Nrf2 pathway by disruption of Keap1 in myeloid leukocytes protects against sepsis, Am. J. Respir. Crit. Care Med. 184 (2011) 928–938.

[9] D.A. Abed, M. Goldstein, H. Albanyan, H. Jin, L. Hu, Discovery of direct inhibitors of Keap1–Nrf2 protein–protein interaction as potential therapeutic and preventive agents, Acta Pharm. Sin. B 5 (2015) 285–299.

[10] P. Vanhee, A.M. van der Sloot, E. Verschueren, L. Serrano, F. Rousseau, J. Schymkowitz, Computational design of peptide ligands, Trends Biotechnol. 29 (2011) 231–239.

[11] G. Wells, Peptide and small molecule inhibitors of the Keap1–Nrf2 protein–protein interaction, Biochem. Soc. Trans. 43 (2015) 674–679.

[12] Y. Chen, D. Inoyama, A.N. Kong, L.J. Beamer, L. Hu, Kinetic analyses of Keap1-Nrf2 interaction and determination of the minimal Nrf2 peptide sequence required for Keap1 binding using surface plasmon resonance, Chem. Biol. Drug Des. 78 (2011) 1014–1021.

[13] D. Inoyama, Y. Chen, X. Huang, L.J. Beamer, A.N. Kong, L. Hu, Optimization of fluorescently labeled Nrf2 peptide probes and the development of a fluorescence polarization assay for the discovery of inhibitors of Keap1–Nrf2 interaction, J. Biomol. Screen. 17 (2012) 435–447.

[14] N. London, B. Raveh, D. Movshovitz-Attias, O. Schueler-Furman, Can self-inhibitory peptides be derived from the interfaces of globular protein-protein interactions, Proteins 78 (2010) 3140–3149.

[15] C. Yang, S. Zhang, P. He, C. Wang, J. Huang, P. Zhou, Self-binding peptides: folding or binding, J. Chem. Inf. Model. 55 (2015) 329–342.

[16] C. Yang, S. Zhang, Z. Bai, S. Hou, D. Wu, J. Huang, P. Zhou, A two-step binding mechanism for the self-binding peptide recognition of target domains, Mol. BioSyst. 12 (2016) 1201–1213.

[17] R. Hancock, M. Schaap, H. Pfister, G. Wells, Peptide inhibitors of the Keap1–Nrf2 protein–protein interaction with improved binding and cellular activity, Org. Biomol. Chem. 11 (2013) 3553–3557.

[18] N.D. Georgakopoulos, S.K. Talapatra, J. Gatliff, F. Kozielski, G. Wells, Modified peptide inhibitors of the Keap1–Nrf2 protein–protein interaction incorporating unnatural amino acids, Chembiochem 19 (2018) 1810–1816.

[19] Y. Katoh, K. Iida, M.I. Kang, A. Kobayashi, M. Mizukami, K.I. Tong, M. McMahon, J.D. Hayes, K. Itoh, M. Yamamoto, Evolutionary conserved N-terminal domain of Nrf2 is essential for the Keap1-mediated degradation of the protein by proteasome, Arch. Biochem. Biophys. 433 (2005) 342–350.

[20] K.I. Tong, B. Padmanabhan, A. Kobayashi, C. Shang, Y. Hirotsu, S. Yokoyama, M. Yamamoto, Different electrostatic potentials define ETGE and DLG motifs as hinge and latch in oxidative stress response, Mol. Cell. Biol. 27 (2007) 7511–7521.

[21] H.M. Berman, J. Westbrook, Z. Feng, G. Gilliland, T.N. Bhat, H. Weissig, I.N. Shindyalov, P.E. Bourne, The protein data bank, Nucleic Acids Res. 28 (2000) 235–242.

[22] F. Tian, Y. Lv, P. Zhou, L. Yang, Characterization of PDZ domain-peptide interactions using an integrated protocol of QM/MM, PB/SA, and CFEA analyses, J. Comput. Aided Mol. Des. 25 (2011) 947–958.

[23] F. Tian, R. Tan, T. Guo, P. Zhou, L. Yang, Fast and reliable prediction of domain–peptide binding affinity using coarse-grained structure models, Biosystems 113 (2013) 40–49.

[24] F. Tian, C. Yang, C. Wang, T. Guo, P. Zhou, Mutatomics analysis of the systematic thermostability profile of Bacillus subtilis lipase A, J. Mol. Model. 20 (2014) 2257.

[25] Y. Duan, C. Wu, S. Chowdhury, M.C. Lee, G. Xiong, W. Zhang, R. Yang, P. Cieplak, R. Luo, T. Lee, J. Caldwell, J. Wang, P. Kollman, A point-charge force field for molecular mechanics simulations of proteins based on condensed-phase quantum mechanical calculations, J. Comput. Chem. 24 (2003) 1999–2012.

[26] D.A. Case, T.E. Cheatham, T. Darden, H. Gohlke, R. Luo, K.M. Merz, A. Onufriev, C. Simmerling, B. Wang, R.J. Woods, The amber biomolecular simulation programs, J. Comput. Chem. 26 (2005) 1668–1688.

[27] W.L. Jorgensen, J. Chandrasekhar, J.D. Madura, R.W. Impey, M.L. Klein, Comparison of simple potential functions for simulating liquid water, J. Phys. Chem. 79 (1983) 926–935.

[28] Y. Yang, H. Liu, X. Yao, Understanding the molecular basis of MK2-p38α signaling complex assembly: insights into protein-protein interaction by molecular dynamics and free energy studies, Mol. BioSyst. (8) (2012) 2106–2118.

[29] C. Yang, C. Wang, S. Zhang, J. Huang, P. Zhou, Structural and energetic insights into the intermolecular interaction among human leukocyte antigens, clinical hypersensitive drugs and antigenic peptides, Mol. Simul. 41 (2015) 741–751.

[30] P. Zhou, S. Zhang, Y. Wang, C. Yang, J. Huang, Structural modeling of HLA-B1502 peptide carbamazepine T-cell receptor complex architecture: implication for the molecular mechanism of carbamazepine-induced Stevens-Johnson syndrome toxic epidermal necrolysis, J. Biomol. Struct. Dyn. 34 (2016) 1806–1817.

[31] T. Darden, D. York, L. Pedersen, Particale mesh Ewald and N.log(N) method for Ewald sums in large systems, J. Chem. Phys. 98 (1983) 10089–10092.

[32] J.P. Ryckaert, G. Ciccotti, H.J.C. Berendsen, Numerical integration of the Cartesian equations of motion of a system with constraints: molecular dynamics of n-alkanes, J. Comput. Phys. 23 (1997) 327–341.

[33] N. Homeyer, H. Gohlke, Free energy calculations by the molecular mechanics Poisson-Boltzmann surface area method, Mol. Inf. 31 (2012) 114–122.

[34] P.A. Kollman, I. Massova, C. Reyes, B. Kuhn, S. Huo, L. Chong, M. Lee, T. Lee, Y. Duan, W. Wang, O. Donini, P. Cieplak, J. Srinivasan, D.A. Case, T.E. Cheatham, Calculating structures and free energies of complex molecules: combining molecular mechanics and continuum models, Acc. Chem. Res. 33 (2000) 889–897.
[35] J. Yu, S. Wang, J. Yu, C. Liu, F. Xu, S. Wang, Y. Yi, Y. Yin, Structure-based rational design of self-inhibitory peptides to disrupt the intermolecular interaction between the troponin subunits C and I in neuropathic pain, Bioorg. Chem. 73 (2017) 10–15.
[36] T. Hou, K. Chen, W.A. McLaughlin, B. Lu, W. Wang, Computational analysis and prediction of the binding motif and protein interacting partners of the Abl SH3 domain, PLoS Comput. Biol. 2 (2006) e1.
[37] Y. Zhang, K. Schulten, M. Gruebele, P.S. Bansal, D. Wilson, N.L. Daly, Disulfide bridges: bringing together frustrated structure in a bioactive peptide, Biophys. J. 110 (2016) 1744–1752.
[38] P. He, D.L. Tan, H.X. Liu, F.L. Lv, W. Wu, The auto-inhibitory state of Rho guanine nucleotide exchange factor ARHGEF5/TIM can be relieved by targeting its SH3 domain with rationally designed peptide aptamers, Biochimie 111 (2015) 10–18.
[39] T. Wu, P. He, W. Wu, Y. Chen, F. Lv, Targeting oncogenic transcriptional corepressor Nac1 POZ domain with conformationally constrained peptides by cyclization and stapling, Bioorg. Chem. 80 (2018) 1–10.
[40] R.C. Tyler, F.C. Peterson, B.F. Volkman, Distal interactions within the par3-VE–cadherin complex, Biochemistry 49 (2010) 951–957.
[41] K.I. Tong, Y. Katoh, H. Kusunoki, K. Itoh, T. Tanaka, M. Yamamoto, Keap1 recruits Neh2 through binding to ETGE and DLG motifs: characterization of the two-site molecular recognition model, Mol. Cell. Biol. 26 (2006) 2887–2900.
[42] T. Fukutomi, K. Takagi, T. Mizushima, N. Ohuchi, M. Yamamoto, Kinetic, thermodynamic, and structural characterizations of the association between Nrf2-DLGex degron and Keap1, Mol. Cell. Biol. 34 (2014) 832–846.
[43] Y. Ren, X. Chen, M. Feng, Q. Wang, P. Zhou, Gaussian process: a promising approach for the modeling and prediction of peptide binding affinity to MHC proteins, Protein Pept. Lett. 18 (2011) 670–678.
[44] P. Zhou, C. Yang, Y. Ren, C. Wang, F. Tian, What are the ideal properties for functional food peptides with antihypertensive effect? A computational peptidology approach, Food Chem. 141 (2013) 2967–2973.
[45] P. Zhou, C. Wang, F. Tian, Y. Ren, C. Yang, J. Huang, Biomacromolecular quantitative structure-activity relationship (BioQSAR): a proof-of-concept study on the modeling, prediction and interpretation of protein–protein binding affinity, J. Comput. Aided Mol. Des. 27 (2013) 67–78.
[46] H. Luo, T. Du, P. Zhou, L. Yang, H. Mei, H. Ng, W. Zhang, M. Shu, W. Tong, L. Shi, D.L. Mendrick, H. Hong, Molecular docking to identify associations between drugs and class I human leukocyte antigens for predicting idiosyncratic drug reactions, Comb. Chem. High Throughput Screen. 18 (2015) 296–304.
[47] P. Zhou, F. Tian, Z. Shang, 2D depiction of nonbonding interactions for protein complexes, J. Comput. Chem. 30 (2009) 940–951.
[48] H. Yu, P. Zhou, M. Deng, Z. Shang, Indirect readout in protein–peptide recognition: a different story from classical biomolecular recognition, J. Chem. Inf. Model. 54 (2014) 2022–2032.
[49] Z. Bai, S. Hou, S. Zhang, Z. Li, P. Zhou, Targeting self-binding peptides as a novel strategy to regulate protein activity and function: a case study on the proto-oncogene tyrosine protein kinase c-Src, J. Chem. Inf. Model. 57 (2017) 835–845.
[50] W. Zhang, B. Zhong, C. Zhang, Y. Wang, S. Guo, C. Luo, Y. Zhan, Structural modeling of osteoarthritis ADAMTS4 complex with its cognate inhibitory protein TIMP3 and rational derivation of cyclic peptide inhibitors from the complex interface to target ADAMTS4, Bioorg. Chem. 76 (2018) 13–22.
[51] P. Zhou, S. Hou, Z. Bai, Z. Li, H. Wang, Z. Chen, Y. Meng, Disrupting the intramolecular interaction between proto-oncogene c-Src SH3 domain and its self-binding peptide PPII with rationally designed peptide ligands, Artif. Cells Nanomed. Biotechnol. 46 (2018) 1122–1131.
[52] M.C. Lu, Z.Y. Chen, Y.L. Wang, Y.L. Jiang, Z.W. Yuan, Q.D. You, Z.Y. Jiang, Binding thermodynamics and kinetics guided optimization of potent Keap1–Nrf2 peptide inhibitors, RSC Adv. 5 (2015) 85983–85987.
[53] M.C. Lu, Q. Jiao, T. Liu, S.J. Tan, H.S. Zhou, Q.D. You, Z.Y. Jiang, Discovery of a head-to-tail cyclic peptide as the Keap1-Nrf2 protein-protein interaction inhibitor with high cell potency, Eur. J. Med. Chem. 143 (2018) 1578–1589.